J Therm Anal Calorim (2012) 109:1117–1132
DOI 10.1007/s10973-012-2326-2

Termination of crystallization or ordering of flexible, linear macromolecules

Bernhard Wunderlich

NATAS2011 Conference Special Chapter

Abstract This review concerns the "termination of crystallization or ordering of flexible, linear macromolecules" before the transition from the amorphous phase reaches thermodynamic equilibrium. It makes use of the precision of hindsight in interpretation of old experiments and the back-integration of more recent experiments into the knowledge gained from the well-known older experiments which had led to the paradox: Once the semi-ordered sample is produced, its disordering frequently follows a zero-entropy-production path, i.e., its latent heat is linked to the free enthalpy of the non-equilibrium phase, while on ordering, there exists a metastable temperature region of the polymer melt which cannot be broken by nuclei of the ordered phase. The classic scheme of crystallization via nucleation and growth is used to set the stage for the discussion. This scheme has been used for many years to describe the motion of single motifs to crystallize small, rigid molecules and its slow-down when approaching the glass transition. For flexible macromolecules, the ordering mechanism needs to be expanded to the description of cooperative ordering schemes of more than one motif of the molecular segments and a more complicated, multiple-step slow down when approaching the much wider glass transition region. The structural features causing the incomplete ordering of flexible macromolecules are the three-dimensional defects created at the phase boundaries between ordered and disordered phases, initially called the amorphous defects. The matter contained in these amorphous defects possesses a much broader glass transition. If this glass transition lies above the glass transition of the unrestrained, amorphous phase, the amorphous defects represent a separate nanophase, called a rigid-amorphous fraction. Modern differential scanning calorimetry (DSC), temperature-modulated DSC, and differential fast scanning calorimetry permit the study of latent heats and heat-capacity changes involved in the liquid–solid transitions of amorphous phases, crystals, and mesophases. In this more complex framework, the "termination of crystallization of flexible, linear macromolecules" is described together with the possibility of molar mass segregation by long-range and local diffusion instead of a thermodynamic mechanism.

Keywords Amorphous defects · Local and cooperative processes · Nucleation · Rigid amorphous fraction (RAF) · Segregation by diffusion · Semicrystalline flexible polymers

Introduction

In the 1950s, the knowledge of crystals and the corresponding melt of *small molecules* was applied to describe also semicrystalline, flexible *macromolecules*, commonly, less precisely, called semicrystalline polymers. We honor Bruce Prime in this symposium who proved in the 1960s with his thesis experiments that a similar equilibrium as expected for crystals of small molecules can, indeed, be approached during melting with specially crystallized polyethylene, PE. This PE was analyzed after first being

The Figs. 1, 2, 3, 4, 5, 6, 7, 8 and 9 in this publication were redrawn and updated with permission from the copyright holder of [1]. The figures: 17-05; 28-54; 9-15; 26-07; 34-39, 49; 16-41, 38; 32-45, correspond to Figs. 1, 2, 3, 4, 5, 6, 7, 8 and 9, in sequence. Similarly, Fig. 10 was redrawn from [8], and Figs. 11 and 12 from [47].

B. Wunderlich (✉)
Department of Chemistry, The University of Tennessee, Knoxville, TN 37996-1600, USA
e-mail: Wunderlich@CharterTN.net

B. Wunderlich
200 Baltusrol Road, Knoxville, TN 37934-3707, USA

crystallized at elevated pressure into its mobile, hexagonal equilibrium mesophase, followed by cooling and pressure-release to obtain orthorhombic equilibrium crystals [2–4]. This special process yields close to 100% crystallinity and produces crystals with largely extended-chain macroconformations. These crystals were grown from melts with different molar masses and mass distributions, and their thermal properties were analyzed by standard differential scanning calorimetry, DSC. The data seemed to agree with the assumption of equilibrium melting, as earlier proposed by Flory [5]. For high-molar masses the melting range was *narrower* than for full segregation, suggesting mixed crystal formation above molar masses of 12,000 Da.

Without this path of ordering via a mobile intermediate mesophase, however, most linear, flexible polymers, including PE, yield *semicrystalline polymers which are metastable*. The metastability is characterized by two major properties: A melting temperature, T_m, which is far below the equilibrium melting temperature, T_m°; and a crystallinity, w_c, which is less than 100%. To understand this metastability, a thermodynamic treatment of the non-equilibrium was attempted [6], and compared to the equilibrium crystals produced as described above and also by the method of *crystallization during polymerization* [7]. The limited equilibrium data were then combined with an extensive literature review of experiments, published in the three-volume treatise on "Macromolecular Physics," completed in 1980 [8]. In 2005, this information was combined with more information from modern thermal analysis in the textbook "Thermal Analysis of Polymeric Materials" [9]. Typical results on rates of crystallization and melting from these wide-ranging experiments are summarized in Fig. 1. The equilibrium behavior is represented in the graph by the point at $\Delta T = 0$ at zero crystallization and melting rates. All curves represent linear rates of changes of crystal dimensions observed by optical or electron microscopy. The crystallization rate curves indicate *supercooling*, the melting rate curves *superheating*, and the intermediate, horizontal segments at zero crystallization rate mark the region of *metastable melt* in the presence of crystals.

Besides the change in T_m°, there is the change of $\Delta T = T_m^\circ - T_m$ arising from the kinetics of the phase transitions. Furthermore, at the crystal-melt interface no crystallization is observed for a supercooling ΔT of typically 5–15 K, indicating the above mentioned region of metastable melt. The limiting w_c on crystallization changes with polymer type and crystallization condition. For its understanding, it was necessary to analyze the order–disorder transition not only by establishing T_m and the corresponding latent heat, but also the heat capacity to assess the *molecular motion* of the chain segments within all phase areas making up the polymer sample. Surprisingly,

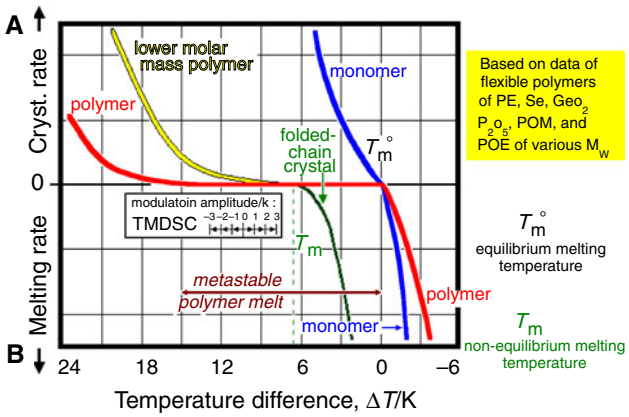

Fig. 1 Crystallization and melting rates and the temperature range of metastable polymer melt observed by microscopy, $\Delta T = T_m^\circ - T_m$. [1, 8, and 9]. (*A*) Typical crystallization rates of high and lower molar mass polymers as well as of a monomer. (*B*) Typical melting rates of monomer, polymer, and of folded-chain polymer crystals

the semicrystalline polymer sample may not only consist of the commonly assumed crystalline and amorphous phases; the amorphous portion must be separated into *mobile amorphous and rigid amorphous* phases. Typically, single polymer molecules contain 1,000–10^7 atoms, and the identifiable phase areas commonly have *microphase* to *nanophase* dimensions.

The modulation amplitudes of temperature-modulated DSC, TMDSC, in frequent use for the last 20 years, are also indicated in Fig. 1. They show the usefulness of TMDSC to test the reversibility of phase changes within semicrystalline polymers. An updated basic description of phases, molecular motion, sizes, and shapes, of semicrystalline polymers is reviewed in the next two "Sections," based mainly on experimental observations [8.9]. This will be followed by the effort to resolve the title problem.

Basic description

As a modern science, *chemistry* had its beginning only about 200 years ago. The essential discovery was the experiment-based proof of the existence of atoms and molecules as the microscopic building blocks of matter [10].[1] At about the same time, an arbitrary division of chemistry into *inorganic* und *organic* was adopted based on the origin of the different types of matter. This distinction was already obsolete some 50 years later when increasing numbers of "organic" sub-

[1] The idea about the atomic nature of matter appeared first in his notes covering 1802/04. The book is frequently reprinted; for example, see: The Science Classical Library. New York: Citadel Press; 1964.

stances could be synthesized out of "inorganic" molecules without "organic" means. Instead of dropping the superfluous subdivision, a further partition was made by introducing *biochemistry* as the "truly organic chemistry." Today, we know that all molecules follow the same principles governing synthesis, structure, molecular motion, composition, and properties. The early arbitrary, historic division, hinders back-integration of new knowledge when gained in one of the separate sub-disciplines and, thus, slows the overall progress of chemistry.

The macroscopic characteristic of matter as perceived by the human senses was categorized already in antiquity. The three clearly different appearances were named: gaseous (air), liquid (water), and solid (earth). Gases are *dilute phases* with its molecules well separated, while liquids and solids are *condensed phases* with touching molecules. A unique combination of the *microscopic nature of matter and its macroscopic characteristics* became possible after flexible macromolecules were recognized in the first half of the twentieth century, representing the last, separate type of molecule.

Since then, one can divide all molecules into three types, namely, *small molecules*, large molecules, and *macromolecules* [11 and 12], with the latter being further divisible into *rigid macromolecules* and *flexible macromolecules* [8, 9]. Less precise, the latter are often just called "flexible polymers." The usefulness of this division lies in the different properties of these three molecule types. Small molecules may be either gaseous, liquid, or solid. Flexible polymers may only be liquid or solid, while rigid macromolecules can only be solid. To reach the "forbidden" states for the macromolecules, they must depolymerize into smaller molecules and, thus, lose their original molecular integrity.

This scheme of phases is shown in Fig. 2 and can be linked easily to (a) The *type of molecules* (small, large-flexible, or large-rigid[2]); (b) their three *macroscopic appearances* (gaseous-dilute, mobile-condensed, and solid); (c) their five different *degrees of disorder* (ranging from "amorphous" to three mesophases ["liquid crystalline" (LC), "plastic crystalline", and "conformationally disordered"], to completely "crystalline"); and (d) the three *phase-sizes* ("macro, micro, or nano"). The *number of condensed phases*, of interest to this discussion, is only 57 [13]. The history and details of this scheme were described at the 37th NATAS Meeting in Lubbock, TX [14].

The disordering transitions between the boxes which represent the different phases in Fig. 2 are marked on the

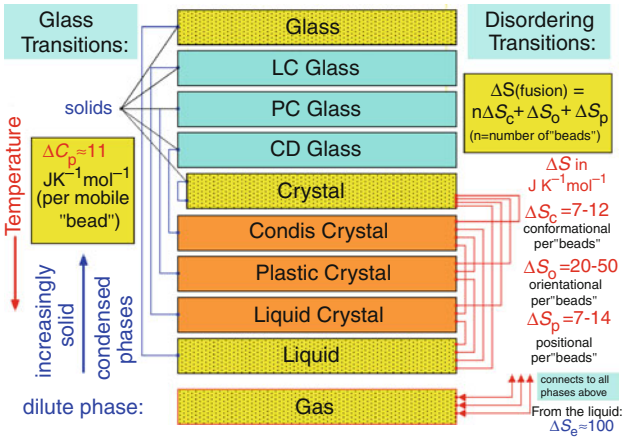

Fig. 2 Subdivision of matter into ten phases based on the three macroscopic appearances (gaseous-dilute, mobile-condensed, and solid) and five degrees of disorder [14]

right side. Their changes in entropy, ΔS_d, can be estimated from the listed typical contributions derived from measurements on many substances. The entropy of fusion, ΔS(fusion), is chosen as an example for the crystal to melt transition (under equilibrium conditions).

The upper five phases in Fig. 2 are designated as solids, as marked on the left side. They are connected to their corresponding lower non-solid phases, occurring at lower temperature, with transitions from the solid state, the glass transition temperature, T_g. At T_g the solids have the identical structure as their corresponding mobile phases. None of these five solids can undergo further ordering or disordering without first leaving the solid state. For example, crystallization of a glass is only possible above its T_g where there is, at least locally, sufficient molecular mobility. Of particular interest is that some crystals can have a glass transition without change in crystal structure, as marked in Fig. 2. In this case, the crystal is considered to be a solid only below its T_g [14]. For many molecules, the glass transition and the disordering transition take place simultaneously, a fact that led to the erroneous assumption that *all* crystals are "solid." In Fig. 2, the typical change in heat capacity per mobile "bead" at the glass transition, ΔC_p, is marked on the left [15].

One should note that for flexible polymers the base unit for the thermodynamic functions, the *bead*, is the portion of the molecule connected to its large-amplitude motion. For example, for PE the "bead" is the CH_2-group, identical to the repeating unit, while for poly(oxyethylene), POE, the repeating unit of (O–CH_2–CH_2–) accounts for three "beads."

Finally, the typical evaporation entropy from liquid to gas, ΔS_e, at fixed dilution, is listed at the bottom right as Trouton's rule [16]. In this case, since the whole (small) molecule is the unit that undergoes the phase change from

[2] The first write-up of the suggested classification of molecules was given in [8] (vol 3, Sect. 8.1.2); 1980. For a detailed discussion of this topic, see also [9], Sect. 2.5.

the condensed (small S) to the dilute phase (large S), ΔS_e is the molar quantity.

The understanding of the microscopic nature of *heat* (the fourth element of antiquity) was gained in the mid-nineteenth century and is linked to the "molecular motion." Matter and heat could thereafter be described by the *functions of state of thermodynamics*.[3] The basic function connecting heat and matter is the thermodynamic energy or internal energy, U, which changes with temperature with $C_{V,n}\,dT$, where $C_{V,n}$ is the heat capacity at constant volume, V, and composition, n. The parallel function at constant pressure, p, is the enthalpy, H, with $C_{p,n}$, being the analogous heat capacity. Thus, molecular energy and motion are connected to the calorimetric $C_{p,n}$, of which large experimental collections exist for over 100 years.

For the *function of state of an ideal gas*, the individual molecules are sufficiently separated so that the overall energy can be assessed by their independent molecular motion [9]. For monatomic gases, $C_{V,n}$ is represented solely by the *translational kinetic energy* of its three degrees of freedom ($C_{V,n} = 3/2\,RT$). For rigid, small molecules of two or more atoms, one must add the kinetic energy of two or three degrees of *rotational freedom* depending on its structure, 2/2 or 3/2 RT. Any additional vibrational degrees of freedom need also be added to the total C_V. Depending on their excitation, each degree of vibrational freedom has a contribution to C_V between 0 and RT for their combined kinetic and potential energy. Finally, molecules which become flexible at higher temperatures change one or more of the vibrational degrees of freedom into *hindered rotations* with commonly initially higher contributions to C_V than the corresponding vibration [17]. As the volume of a gas or the temperature decreases, a condensed phase is approached. The gas loses its "ideal" character and the potential energy of interaction between the molecules must be evaluated.

The condensed phases listed in Fig. 2 can be characterized as states where the neighboring molecules are in contact. When lowering the temperature (moving upward in Fig. 2) the phases increasingly lose their *large-amplitude mobility* which, depending on structure, can consist of translation, rotation, and hindered rotation. Ultimately, this change leads to the solid state (at T_g, left side of Fig. 2) [18]. Before reaching T_g, this change in mobility can also change the degree of order, as marked on the right side of Fig. 2.

[3] See, for example, Gibbs JW: On the equilibrium of heterogeneous substances. Trans Conn Acad 1875–78;III:108–248 and 343–524. An extended abstract was published in Am J Sci Ser 3 1878;16:441–458, all reprinted in Bumstead HA, Gibbs van Name R: The scientific papers of J. Willard Gibbs, vol 1, thermodynamics. New York: Dover Publ; 1961.

The *molecular motion in all solids* is mainly vibrational. In the early twentieth century, small molecules and rigid macromolecules were the major solid compounds investigated. Two simple approximations of the vibrational $C_{V,n}$ of such solids were established by Einstein [19] and Debye [20]. The distinction between liquids and solids was at that time linked to the melting of crystals of small molecules (like ice) or rigid macromolecules (like metals, minerals, or salts). These types of melts are usually very mobile. Melts close to their glass transition, T_g, in contrast, have much higher viscosity. Based on the knowledge of the unchanging structure at T_g, disregarding its changes in mobility, glasses were at that time called supercooled "liquids," an erroneous designation that unfortunately is occasionally still in use today [18].

The first extensive review and tabulation of $C_{p,n}$ of *molecular motion of flexible macromolecules* was published in 1970 [21]. Figure 3 illustrates the analysis for PE [9]. The vibrational C_V consists of two major contributions, *skeletal and group vibrations*. The two skeletal vibrations of PE are determined by the weak forces between the molecules and the strong forces along the chain molecules. They can be approximated by the Debye frequency Θ_3, a three-dimensional function, and a one-dimensional Debye function, characterized by the frequency Θ_1. The higher group-vibration frequencies are linked to the local molecular structures (A and B in Fig. 3). The vibrational $C_{V,n}$ of the glass and crystal are similar, except for a somewhat lower Θ_3 for the glass. For the glassy PE, Θ_3 is 80 K, compared to 158 K for the crystal.

At T_g, the difference between the experimental heat capacities at constant pressure of the liquid and solid is ΔC_p. In PE, the mid-point of the glass transition is located at 237 K with a ΔC_p of 10.5 J K^{-1} (mol CH$_2$)$^{-1}$, close to the value expected for its number of "beads" listed in Fig. 2. The glass transition range of fully amorphous polymers is typically only 5–20 K [9]. But for PE, the gradual increase of C_p begins already at 120 K. Due to the structure of PE, this gradual increase of C_p could be linked to the local *cis–trans*, *large-amplitude motion* [22]. The data for PE prove that the key motion for the glass transition begins with such local motion, which gets excited gradually over a large temperature range ($\approx$120–220 K) and completes its excitation at higher temperature with a more abrupt change of its cooperative motion (220–250 K) [21, 22]. Such broadening of the glass transition in polymeric samples will be shown below to be common, explaining many phenomena unique for semicrystalline, flexible polymers. As in PE, it can stretch the beginning of the T_g to lower temperature due to localized large-amplitude motion, it can, however, also stretch the end of the T_g to higher temperatures by hindering the large-amplitude motion close to boundaries to a more rigid phase or by

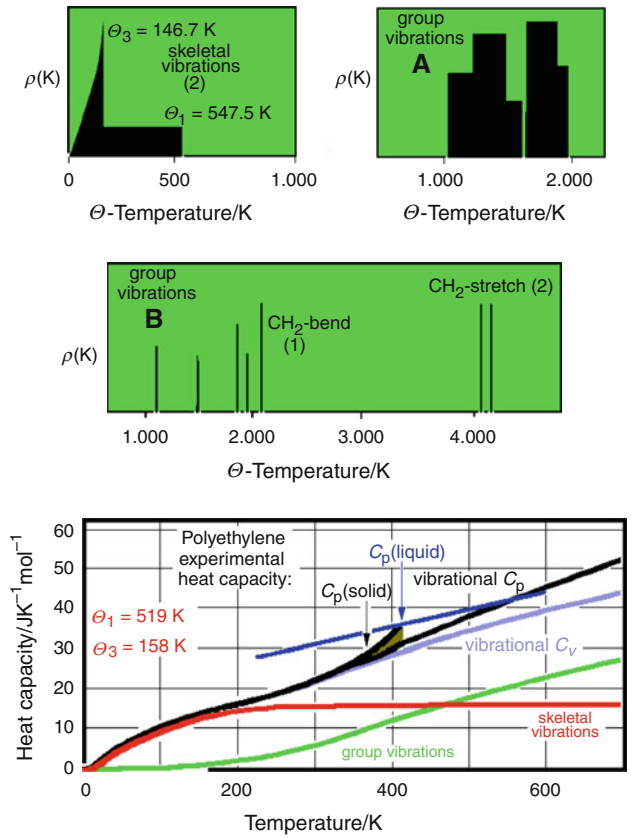

Fig. 3 Vibrational spectra (*top three diagrams*) and the contributions of the vibrations to the C_V and C_p of crystalline PE (*bottom curves*) [1, 9, and 21]. The Θ temperatures refer to the temperature at which the corresponding vibration frequency is largely excited, i.e., $C_V \approx R$. The densities of vibrational states are represented by ρ(K). The conversion factor from the Θ temperature to the corresponding frequency are 1.0 K $\equiv 2 \times 10^{10}$ Hz ($\equiv$0.70 cm^{-1})

applying external strain, as in drawn fibers. Both of these latter restraints may produce a *rigid amorphous fractions* (*RAF*) [18]. The *ATHAS Data Bank* provides the thermodynamic function for many polymers for such analysis [23].

Finally Figure 4, illustrates four basic *macroconformations* proposed in the early years of research in macromolecular physics ([8] Sect. 3.2.1). The term "macroconformation" was chosen to characterize the macromolecule as a whole, rather than a local conformation or configuration.[4] To get an approximate feeling for the dimensions involved, one can look at a typical linear PE molecule consisting of 20,000 CH_2-groups, which has a molar mass of $\approx$280,000 Da. It reaches a length of 2.5 μm when fully stretched and a mean-square, end-to-end distance of 52.9 nm [9]. On ordering such an amorphous macroconformation, one expects, at least initially, a "micellar structure," indicated as state D in Fig. 4. As mentioned in the "Introduction," the equilibrium crystals require an extended-chain macroconformation, C, as proven by thermal analysis. The amorphous melt, however, does not have a direct path from its state A to C. A *chain-folding principle* was suggested in [8], Sect. 3.2.2.1, to account for this observation and was described as follows: "A sufficiently regular, flexible macromolecule crystallized from the mobile random state will always crystallize first in a folded-chain macroconformation" (represented by state B and possibly D in Fig. 4). Once these intermediate states are reached, annealing to more regular and increased fold lengths and higher crystallinities can occur. The mechanism of the movement of a chain through the crystal could be visualized by molecular dynamics simulation, as is reviewed with Figs. 17–20 in [24]. Such increase in fold length is enhanced considerably when the sample is ordering into the more mobile, LC or condis crystalline states of Fig. 2. In fact, except for "crystallization during polymerization" from suitable monomers [7], all extended-chain, flexible polymer crystals known to date were produced by initially ordering in one of the more mobile mesophases, as described in Sect. 5.5 of [9].

The first cause of metastability of folded-chain polymer lamellae is due to their macroconformation, ℓ, the fold length, being typically only between 5 and 50 nm. Such thin lamellae are considered to be *microcrystals*. Compared to large crystals (*macrocrystals*), the enthalpy of microcrystals must be corrected for their surface free energy. Experimentally lamellar PE has a 50–5 K lower T_m than the equilibrium T_m°, respectively, and can be represented by the Gibbs–Thomson equation: $T_m/T_m^\circ = (1 - 0.624/\ell)$ [6 and 8]. The

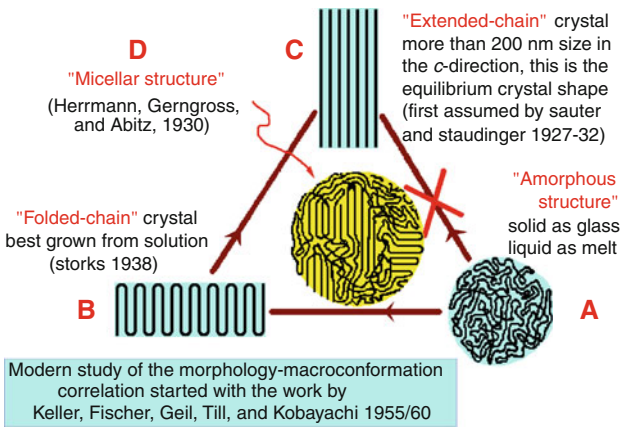

Fig. 4 The macroconformations of flexible chain molecules [8]. The "chain-folding principle" forbids the A → C transition (for references see [9], Fig. 5.42)

[4] One distinguishes a conformation (Latin *conformātĭō*, forming, fashioning) from a configuration (Latin *configĕre*, to join together). Different conformations of a molecule can be attained by rotation about bonds. Configurations need breaking of chemical bonds, as in the attainment of stereo isomers. Wunderlich [1], Fig. 4.41, or [9], Appendix 14, Fig. 3. Note the frequent misuse of these two terms in the common polymer physics literature.

introduction of the folded-chain macroconformations, even if done in crystallographic register, introduces a considerable increase in the surface free energy. Typical side-surface and fold-surface free energies derived from the study of the crystal growth kinetics of PE, for example, are 0.5 and 5.0 μJ cm^{-2}, respectively [9].

The second cause of metastability is the incomplete crystallization. Such structure is obvious for macroconformation D in Fig. 4. Typically observed crystallinities of a semicrystalline sample are 50 ± 20%, but may range sometimes from only a few percent to, rarely, >90%. This reduction in crystallinity was initially linked to *amorphous crystal defects* [25] as discussed in Sect. 4.3.1 of [8]. Analyzing the different macroconformations by thermal analysis, one finds that the "amorphous defects" can be quantitatively identified by their causing a change in the glass transition. The restraint created by the ordered phase and the "entanglements" in the disordered phase, cause an increase in T_g beyond that of the unrestrained melt. This sets up a separate, disordered nanophase called a RAF [9 and 26]. This classification of the amorphous defect as a "nanophase" was based on the understanding of very small microphases which show largely different properties from microphases [13 and 14].

Next, the updated description of matter based on molecular structure, order, motion, and the macroscopic characteristics will be used to improve the discussion of a number of selected experiments on order/disorder transitions of semicrystalline polymers. Many of their major properties were in the past often neglected and can now be linked to the RAF and the molecular motion (and diffusion) effects. The RAF introduces a different phase structure, while the local and long-range molecular diffusion have a strong influence on the rate of the order/disorder transitions.

Experimental observations

Analysis of extended-chain crystals

The transitions of extended-chain crystals of PE, produced as described in the "Introduction," have not only been studied by molar mass determination [2] and electron and optical microscopy [4, 27], but also by thermal analysis using dilatometry [3], DSC [4], and TMDSC [28]. Some results of these experiments are shown in Figs. 5 and 6. In Fig. 5, the orthorhombic crystallinity, w_c, of pressure-crystallized, extended-chain PE is plotted as it decreases on heating slowly at atmospheric pressure through the melting range (6–100 h per recorded point). At low temperature, all samples have a w_c of 96–98%, close to the level expected for full (equilibrium) crystallization. The low-molar mass sample, A, remains close to equilibrium throughout the whole melting range, as marked by the calculated drawn-out curve. Samples B and C are of higher molar mass and broader distributions. They also follow the equilibrium curves, but only at the lower temperatures. Toward higher temperature, they melt more sharply than expected for full segregation into separate crystals on crystallization. The conclusion from this observation was that the molecules of higher molar mass consist of solid-solution crystals [3]. The distribution of the thickness of the extended-chain lamellar crystals as observed by electron microscopy [2], agreed with a segregation of the lower mass molecules, assuming the seen lamellar thickness is equal to the molecular length. During heating, low-molar mass crystals melted quickly, while solid solutions melted slowly, needing dilatometry to avoid superheating [29]. Furthermore, the mechanism of melting of the extended-chain crystals could be seen to involve sequential peeling off layers from the growth faces [4].

Quantitative DSC combined with modern TMDSC permitted a check on the reversibility of the melting. The data are seen in Fig. 6 for sample C in Fig. 5. The standard DSC curve in Fig. 6 shows some superheating which was also studied by dilatometry [4] and fast calorimetry [29]. The small, multiple melting peaks at lower temperature are due to low-molar mass fractions, as also identified in Fig. 5. Each of the 64 quasi-isothermal TMDSC experiments, marked by the circles in Fig. 6, was run for 20 min with sinusoidally alternating sample temperature of amplitude, A, before observing the apparent heat capacity [28]. Except for a minor amount of the lower melting sample, none of the extended-chain crystals melt reversibly. The quasi-isothermal TMDSC signal contains practically only heat capacity contributions and no latent heat. The switch of the samples in Fig. 5 from segregated molar masses to solid solution crystals on crystallization occurred rather sharply at a molar mass of ≈12,000 Da [2, 3].

Limits of reversibility as a function of chain length

Full reversibility of melting and crystallization is known for short-chain paraffins. This is in contrast to the extended-chain crystals of PE seen in Figs. 5 and 6. Since the paraffins can be taken as a model of PE, it is interesting to find the limit of reversibility with chain length, x. The experimental results are displayed in Fig. 7, measured with quasi-isothermal TMDSC with a modulation amplitude $A = 0.5$ K und a modulation period of 60 s [30, 31]. Above $x \approx 75$, i.e., a molar mass of ≈1,000 Da, a sizeable supercooling was necessary for crystallization as indicated earlier in Fig. 1. This limit is much smaller than the chain length for segregation of extended-chain crystallization under pressure for samples A–C of Fig. 5.

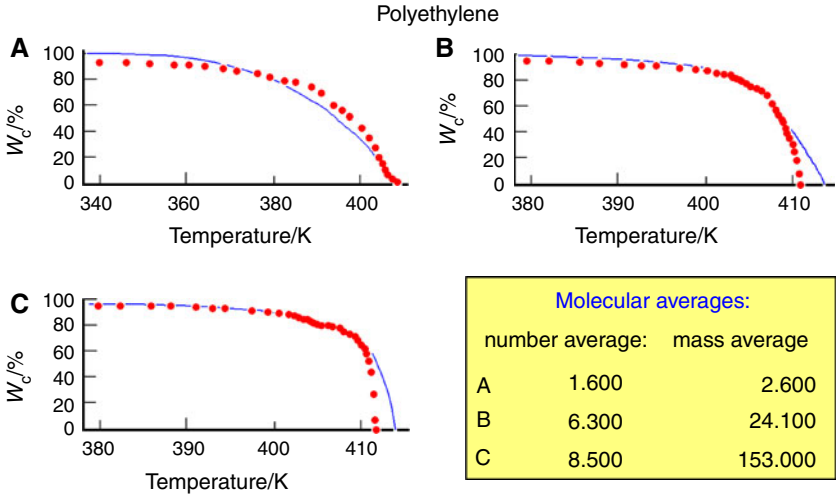

Fig. 5 Slow dilatometry of extended-chain PE at atmospheric pressure to avoid superheating [3]. Mass averages given in g mol^{-1}

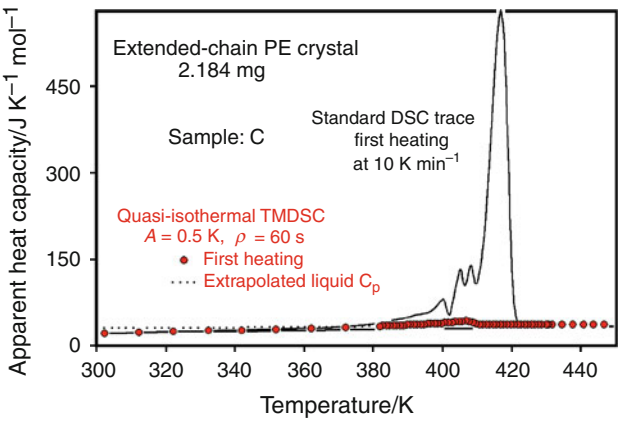

Fig. 6 DSC and quasi-isothermal TMDSC traces of extended-chain PE [4, 28]. The sample analyzed corresponds to sample C shown in Fig. 5

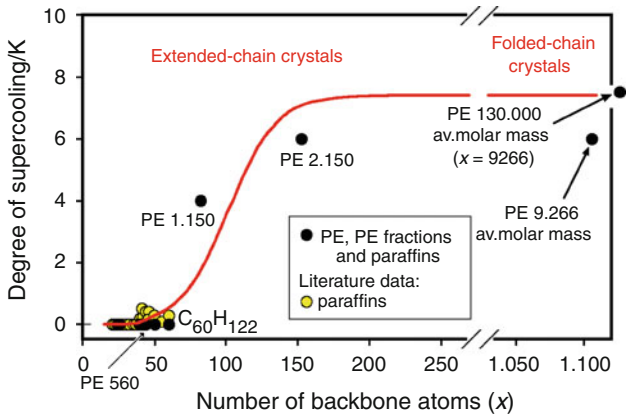

Fig. 7 Supercooling on crystallization of paraffins and folded-chain PE in the presence of crystals as a function of backbone length [30, 31]

During the past 20 years, a small amount of reversible melting was shown, however, for a larger number of different, semicrystalline polymers as long as the sample was not completely melted [32]. Based on the available thermodynamic data of PE, the following picture seems likely for the small amount of reversible melting: A small amount of folded-chain crystals of macroconformations B or D in Fig. 4 can melt reversibly even in the metastable temperature range of the melt indicated in Fig. 1. This reversibility exists as long as the melting chain segment is still attached to the crystal. The reversibility is lost as soon as the temperature modulation exceeds the melting temperature of the overall molecule, or at least melts the *molecular nucleus* to which the reversibly melted chain portion is attached to. Other indications of the existence of a "molecular nucleus" are discussed in the next paragraph. Once the crystal or molecular nucleus are melted, crystallization can only be recovered with the supercooling indicated in Figs. 1 and 7.

Analysis of folded-chain crystals

Extensive studies of crystallization of chain-folded PE are summarized in Fig. 8. They involve the effect of molar mass distribution of supernatant melts or solutions on the distributions of molar mass in the crystals [33–35]. The segregation of the molar masses is shown by curves "1" and "2" for melts and solutions as a function of the melt and solution temperatures, respectively, plotted at the bottom and top temperature scales. At high crystallization temperatures, the segregation far exceeds the equilibrium expected from curve "3," which was calculated from the phase diagram developed in [3].

The maximum in segregation of molar mass reaches ≈20,000 Da, somewhat higher than the ≈12,000 Da for the pressure-crystallization found in Fig. 5. An explanation of this factor of two from Fig. 5 could be the lesser mobility in the melt on crystallization under pressure. Overall, a likely non-thermodynamic cause for the

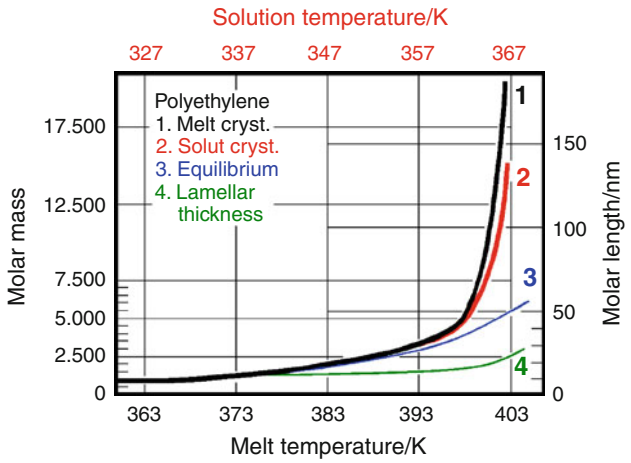

Fig. 8 Upper limit of molar mass left in the melt or in solution on crystallization of chain-folded PE at the corresponding temperatures from broad molar mass distribution samples

segregation may be the different times needed for diffusion of molecules of different lengths to or from the crystallization sites. Once at a given crystal surface, a longer amorphous molecule may (co)crystallize quicker using local diffusion, while a shorter molecule may more quickly diffuse away from the crystallization site before crystallizing sufficiently to be immobilized.

Tie-molecules to neighboring crystals could be identified by DSC by partial melting and proving that not all molten chains could be removed [36]. Tie molecules could also be removed by chemical etching to study the changed molar mass distribution. Based on such experiments, "molecular nucleation" was proposed as a hypothetical barrier for crystallization below T_m° on the crystal surface [35].

The *fractionation governed by thermodynamics* is displayed in Fig. 1 for the example labeled "monomer." To understand the process, one assumes that the melt contains two monomer species "a" and "b" with the equilibrium melting temperature T_{ma}° being lower than T_{mb}°. Adding, then, species "a" by fluctuation to a crystal at the higher equilibrium melting temperature T_{mb}° is frustrated by its faster rate of melting. As long as the crystallization and melting rates extrapolate with *finite slopes* to their respective $\Delta T = 0$, this process leads to segregation, i.e., the higher melting species "b" is kept in the crystal once it is added, while the lower melting "a" accumulates in the melt. For polymers, the crystallization rates in Fig. 1 extrapolate to *slope zero* when reaching $\Delta T = 0$. Once lower and higher molar mass molecules end up on the same crystal surface, reversible fluctuations do not occur. Molecular nucleation must first be overcome, and melting cannot take place unless the temperature is raised to T_m°, i.e., no thermodynamic segregation is possible.

RAF or amorphous defects

The "RAF" is the third phase in semi-ordered polymers, a nanophase, as mentioned in the "Basic Description." The other two phases are the ordered phase (crystal or mesophase) and the "mobile amorphous fractions, MAF." In chain-folded, ordered samples the latter two phases are usually of microphase dimensions. A general, thermodynamic description of such three-phase samples is discussed in [37]. The RAF and the MAF have different glass transitions. Below the T_g(MAF) all three phases are solid. The crystals or mesophases, finally, disorder at T_d with a latent heat absorbed over a temperature range rather than at a sharp transition temperature. For polymers, T_d is usually characterized by the peak of the endotherm, the temperature of fastest disordering at the given analysis rate, T_p. For most semicrystalline polymers the devitrification of the RAF occurs before or during crystal melting [32].

The crystals, RAF, and MAF of poly(oxy-2,6-dimethyl-1,4-phenylene), PPO, in Fig. 9 demonstrate an exceptional behavior, namely that melting can also be influenced by T_g of the RAF [38 and 39]. The T_g(RAF) of semicrystalline PPO stretches from 490 to 510 K (filled circles), while the T_g(MAF) of fully amorphous PPO begins at ≈480 K (open circles). From the heat of fusion of the standard DSC trace in Fig. 9, one can derive a crystallinity of ≈30% below ≈480 K. The measured C_p by DSC and TMDSC suggests that there is no MAF in the semicrystalline sample, all 70% amorphous material is RAF. Inspection of the quasi-isothermal TMDSC shows also that there is no reversibility of melting. After every TMDSC measurement (filled circle), the remaining crystallinity was additionally measured by continuing a standard DSC trace. With this remaining w_c, one can then calculate a hypothetical semicrystalline C_p by assuming that all amorphous phases were MAF. This hypothetical C_p is marked as +++ in Fig. 9.

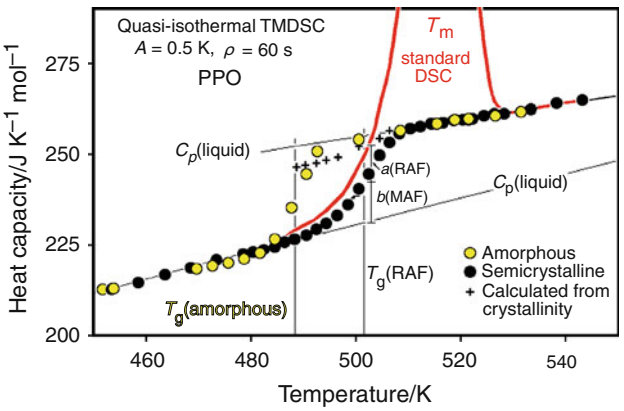

Fig. 9 Apparent heat capacity measured by standard DSC and by quasi-isothermal TMDSC of amorphous (*open circles*) and semicrystalline PPO (*filled circles*)

These data show that on heating of the semicrystalline PPO to 503 K, the amount *a*(RAF) must have remained rigid, and *b*(MAF) was devitrified. From these measurements one can conclude that the RAF devitrifies *before* melting with a rate three times larger than melting. First three repeating units of RAF devitrify before one crystalline repeating unit melts. For PPO, the T_g(RAF) governs the melting contrary to most other polymers.

This exceptional coupling of melting with the glass transition could be further clarified by annealing experiments [39]. Before analysis with standard DSC, on annealing of the semicrystalline PPO at $\approx$503 K, one finds the common increase of T_m (from 517 K before annealing, to 528 K when extrapolated to long annealing times). But, as the melting peak shifts to higher temperatures, it deceases in magnitude. At the 503 K annealing temperature, the subsequent melting peak has disappeared(!) after 600 min. On subsequent cooling the sample does not recrystallize, and on reheating, the annealed sample shows only the T_g(MAF) in Fig. 9 (open circles). Melting of unannealed PPO crystals without the presence of RAF should thus occur at least 20 K below the T_m as seen in Fig. 9, and there is no crystallization on cooling below the T_g(RAF). One can speculate that any crystal nucleus produces so much RAF to stop further crystallization.

For many flexible, semicrystalline polymer molecules, the ratio of T_m/T_g(MAF) is between 2.0 and 1.5 ([9] Sect. 2.5.6). The special behavior shown in Fig. 9 for PPO chains, thus, is caused by the sufficiently rigid nature of its chains to change this ratio to $\approx$1.0. For flexible polymers, like PE, the influence of the crystals on the amorphous phase only broaden the T_g without producing an identifiable separate RAF nanophase, but the mobility is still sufficiently affected so that one could distinguish by electron-spectroscopic imaging a less mobile, noncrystalline layer around every crystal [40]. These and many other TMDSC experiments reveal that a full understanding of ordering and disordering of semi-ordered polymers needs the study of the interactions between the ordered and amorphous microphases as well as the properties of the RAF.

Crystal nucleation

Experiments investigating the nucleation of ordering of flexible macromolecules also led to distinctly different behavior than observed for nucleation involving motifs (the crystallizing species) of small molecules [8 and 41]. In case the amorphous molecules can initiate ordering without the help of earlier structure changes in the melt, the crystallization is said to begin with *homogeneous nucleation*. Homogeneous nucleation becomes possible below a relatively well defined temperature, T_h, and leads to large numbers of ordered entities initiated randomly anywhere in the remaining bulk melt. Before ordering can commence, the positive free enthalpy barrier of a critical nucleus must be overcome by random fluctuations. A common method to assess homogeneous nucleation is to study ordering in sufficiently small droplets so that only a negligible number of droplets can contain any other accidentally present active (heterogeneous) nucleation site. Typical supercooling for flexible polymers, expressed by $T_m^\circ - T_h$, was found to range from 50 to 150 K [8].

Heterogeneous nucleation involves pre-existing ordered surfaces, usually out of foreign materials which permit epitaxy with a lesser free energy barrier than homogeneous nucleation. Heterogeneous nucleation may typically initiate polymer crystallization at supercoolings of only 20–50 K [8].

Self-nucleation is the third type of nucleation. Both, high and low-temperature self-nucleations have been suggested ([8], Vol. III, Sect. 5.1.4). The self-nuclei were found to remain after heating crystals *above* their dissolution or melting temperature and after seemingly all latent heat has been absorbed. After self-nucleation, one observes an ordering temperature, T_c, on cooling above or below T_h for high or low-temperature self-nucleation. Besides, not possessing a measurable latent heat, self-nuclei are limited in number and survive heating above the T_m° for measurable temperature and time limits. Self-nucleation has been assessed by counting the nucleated crystals by optical or electron microscopy. For solutions of PE, it was found that the number of self-nuclei depends on the temperature reached after melting, but not the subsequently chosen T_c. Their nature could be identified as a nodular entity out of which single lamellar crystals grew, but with a much smaller thickness than the nodule [42, 43]. Crystals of higher molar mass can be heated to higher temperature and, thus, produce a certain degree of segregation. Finally, the number of self-nuclei increases with the perfection of the crystals they originated from.

Figure 10 illustrates all three types of nucleation on the example of isotactic polystyrene melt, iPS [44]. The iPS crystals grow relatively slowly, so that the nucleation could be observed by slow dilatometry. On cooling or heating (with rates of 35–75 K min^{-1}) no crystallization occurs along the dash-dotted lines "1" and "2" in the marked directions. The solid lines mark the numbers of nuclei measured after stopping the quenching or heating for 5 min or longer for nucleation. The nuclei were counted after quickly heating or cooling after the stopping to a chosen analysis temperature of 433 K. At this temperature the nuclei grew into visible crystals. The experiments for curve "1" were started at 518 K with a melt containing heterogeneous and self-nuclei. Quenching below $\approx$430 K, the temperature-range of homogeneous nucleation, T_h, is reached. The value of T_h was also measured with droplet experiments on different iPS samples (411 K [45]).

Below 430 K the number of nuclei counted in Fig. 10 increases beyond the original heterogeneous and high-temperature self-nuclei (10^6–10^7 cm^{-3}). The homogeneous nucleation of 10^7–10^9 cm^{-3} increases until the T_g is approached ($\approx$373 K). Additional *low-temperature homogeneous nuclei* are created below this temperature. All added nucleation stops at $\approx$350 K at a number of $>10^{11}$ cm^{-3}.

To analyze the stability of the low-temperature nuclei, curve "2" was followed. The nuclei were produced at 293 K and then brought by quick heating *above* the "temperature region for growing of nucleated crystals." After stopping the dilatometer at higher temperatures, these samples were again cooled quickly to 433 K to count the crystals growing out of any remaining nuclei. Above 500 K the nuclei decreased in number. Above 520 K, the originally present high-temperature self-nuclei at the start of the experiment at 518 K are also destroyed. Finally, above 540 K, only heterogeneous nuclei remain ($<10^6$).

The recently developed differential fast scanning calorimetry, DFSC, with rates of temperature changes of up to 50,000 K s^{-1}, allows freezing of unstable intermediate states during nucleation, ordering, annealing, and melting for later analysis [46]. Figure 11 illustrates a series of such DFSC traces of poly(ε-caproic acid), PCL [47]. All analyzed samples were produced within a chip calorimeter by cooling to 100 K from the melt at the indicated rates. This was followed by analysis of the samples with a heating rate of 1,000 K s^{-1}, as reproduced in Fig. 11. The 1,000 K s^{-1} DFSC allows the study of (a) the glass transition of the cooled samples, (b) the cold crystallization through measurement of the exothermic latent heats, and (c) the melting of crystals grown during cooling and on cold crystallization through their endothermic heats.

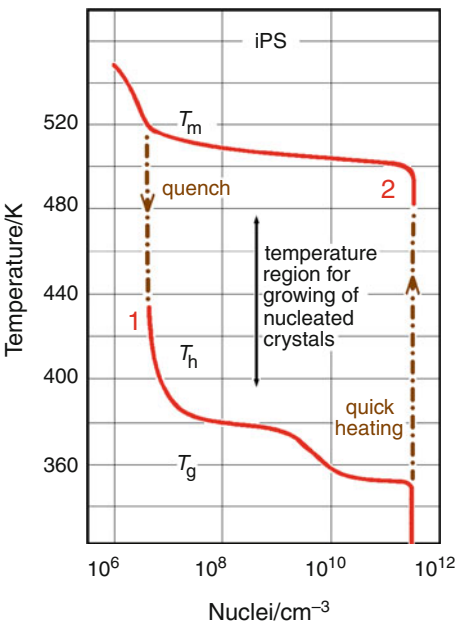

Fig. 10 Determination of the different types of nuclei of iPS measured by counting of crystals. Curve "1", quenching the melt from 518 K and measured after subsequent heating to 433 K. Curve "2", measured after first heating samples that were prior nucleated at 293 K and measured on subsequent cooling to 433 K. Redrawn after [8] Fig. V.30, Vol. II. Data derived from [44]

The slowest cooling rates produce the highest w_c and the smallest ΔC_p at T_g. Due to RAF formation, the glass transition is broadened and shifted to higher temperatures. For the slowest cooling rate, nucleation followed by crystallization was completed already during the cooling step, so that there occurred no cold crystallization during the subsequent analysis. As the cooling rates increase, less crystallization occurs during cooling, and increasing cold crystallization can be seen on heating. With this increasing cooling rate, frozen homogeneous nuclei are created on cooling which first not only increase the exotherm, but also move it to lower temperature. Then, both trends reverse as the number of nuclei decreases and growth moves to higher temperature. On cooling at the maximum rate of 50,000 K s^{-1} the exotherm of cold crystallization equals the endotherm of fusion. Under these conditions no homogeneous nuclei were grown on cooling anymore, only the originally present heterogeneous nuclei initiate cold crystallization. Self-nuclei were eliminated in these experiments by sufficiently high heating (to 470 K) before cooling [47].

Figure 12 shows a summary of experiments for PCL, as described in Fig. 11, but gained from a more structured DFSC application. Samples of $\approx$20 ng melt were cooled at 10,000 K s^{-1} from 470 K ($\approx$100 K above T_m°) down to 100 K ($\approx$100 K below T_g). The samples, containing then only heterogeneous nuclei, were quickly heated to different temperatures for nucleation and crystallization for times, t_c, from 10^{-4} to 10^5 s, followed subsequently by heating for

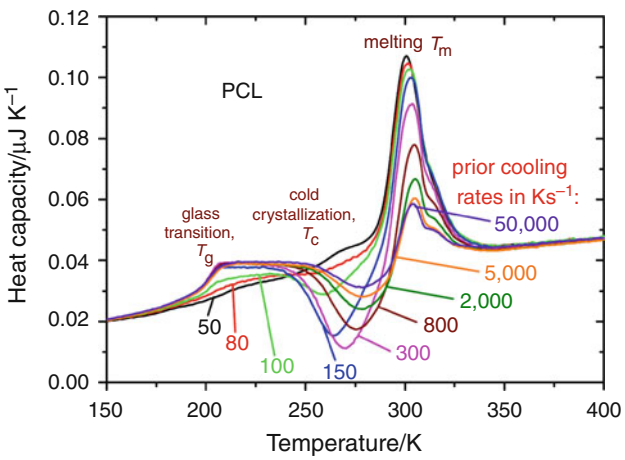

Fig. 11 Melting of PCL, measured by DFSC at 1,000 K s^{-1} after prior cooling the melt to 100 K with rates for 50–50,000 K s^{-1} to determine nucleation and crystallization. Data from [47]

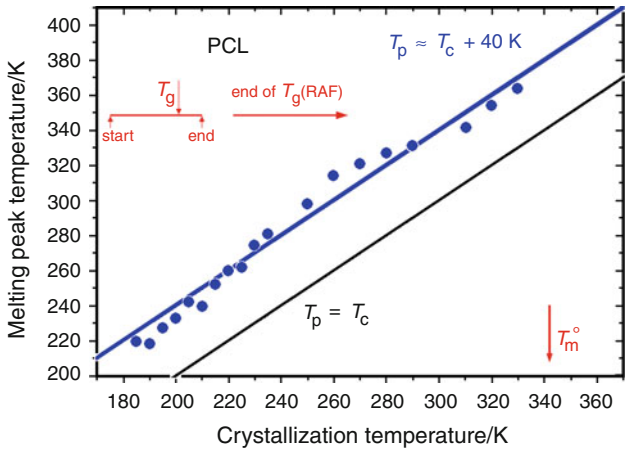

Fig. 12 Melting peak temperatures, T_p, of PCL after crystallizing from the melt at T_c until a constant T_p was reached. Analyzed by DFSC at 1,000 K s^{-1} as in Fig. 11. Data from [47]

analysis with 1,000 K s^{-1} as before in Fig. 11. After completion of the experiment, the nucleation effect on cold crystallization, the change in the glass transition, ΔC_p and T_g, and the final melting of all crystals in the sample was measured. For $t_c < 1$ ms no additional growth of nuclei or crystals occurred at T_c. The ΔC_p and T_g was that of the MAF. Latent heats were only caused on analysis at 1,000 K s^{-1} by cold crystallization of the heterogeneous nuclei (exotherms) and their subsequent fusion (endotherms), similar as seen in Fig. 11 after cooling with 50,000 K s^{-1}.

The Fig. 12 displays next the peak temperatures, T_p, after sufficiently long t_c to complete all isothermal crystal growth at T_c as well as on subsequent cold crystallization. The temperature of cold crystallization induced during the analysis at 1,000 K s^{-1} decreased from 290 K, when only the original heterogeneous nuclei were present, to 240 K, when the first homogeneous nuclei were produced at 185 K. Note that 185 K is also the beginning of T_g. Out of the large number of $\approx$500 experiments, both, growth rates of nucleation and crystallization could be generated and used to infer the progress of low-temperature nucleation and crystal growth [47].

Solutions

Shortly after flexible polymers were established as the third and last type of molecules, their macroconformations were characterized as shown in Fig. 4. By the 1970s, their unique crystallization rates of Fig. 1 were established. Molecular motion was then linked to the thermodynamic functions, as shown in Fig. 3, and the expanded scheme of phases of Fig. 2 could be developed. It was obvious when attempting to crystallize the amorphous macroconformations A in Fig. 4, that its completion is hindered by the formation of amorphous defects or RAF. It was apparent that when cooling toward the glass transition, the diffusion of the molecules as a whole slowed down before the local, large-amplitude, conformational motion of its segments stopped. These details of the hindering of ordering of flexible polymers will be attempted to be resolved in this "Section" using the review of the experiments displayed as Figs. 5, 6, 7, 8, 9, 10, 11 and 12.

Thermodynamics of melting and crystallization

The melting of PE after crystallization under pressure is summarized in Fig. 5. It documents the possibility of equilibrium melting of polymers. The crystals were in equilibrium before being analyzed, i.e., they were close to 100% in crystallinity and of extended-chain type (macroconformation C in Fig. 4). These equilibrium crystals could, however, not be produced by cooling from the melt or solution, as is possible for many small molecules. Owing to the "chain-folding principle" discussed with Fig. 4, the equilibrium state C for polymers must be reached via the metastable macroconformations B and D and a semicrystalline intermediate. The equilibrium crystals of PE had to be reached by a multi-stage, irreversible path. This path was enabled by the higher molecular mobility in the mesophase of PE than in the atmospheric-pressure orthorhombic phase and the chain folds were extended in an annealing step following the crystallization.

Figure 7 illustrated that true equilibrium melting *and* crystallization for PE stops at a molar mass of <1,000 Da. How was it then possible to segregate molar masses up to $\approx$12,000 Da on crystallization under pressure to agree on melting with a multi-component equilibrium phase diagram? Figure 8 shows that the crystallization from the melt and solution of PE produces even larger segregation, despite being far from equilibrium. A possible assumption for this process is a restriction of molecular nucleation, a process based on hindered mobility leading to ordering of longer molecules instead of the different thermodynamic driving forces of the molecules of different length. The semicrystallinity and chain folding seems little affected by the molecular nucleation and is common for most flexible polymers.

The *first part of the* "*Solutions*" leads to the conclusion that the ordering of polymers is irreversible, as illustrated by Figs. 1, 6, 7, and 8. Only a small amount of local reversibility exists, which involves only parts of appropriately crystallized chains, as reviewed in [32]. The melting can usually be documented by proper thermal analysis at its zero-entropy-production limit as described by irreversible thermodynamics. Equilibrium thermodynamics, which describes the equilibrium zero-entropy-production process on melting, does not apply to the crystallization process (see [6] and, for example, Sect. 2.4 of [9]).

Structure, nucleation, and growth of semicrystalline samples

Checking the glass transition of the RAF of macromolecules of different structure and flexibility, a large variation of properties has been discovered [32]. These range from simple broadening of the glass transition from that of the bulk-amorphous phase, as in PE, to the creation of a separate RAF nanophases without overlapping with the MAF, as in poly (butylene terephthalate) [48], to finally, a single non-crystalline phase consisting only of RAF, as shown in Fig. 9 for PPO. In Fig. 9 it was demonstrated that not only does the RAF limit the possible crystallinity, but also the melting was governed by the T_g(RAF) and the T_m could be moved above the equilibrium melting temperature, T_m° . A comparison of PE, isotactic polypropylene (iPP), and isotactic poly(1-butene) (iPB) shows the influence of chain mobility on the properties of the semi-ordered states [49]. In the past, semicrystalline polymers were characterized by their chemical and crystal structure and the thermodynamic quantities T_m, T_m° , w_c, and T_g. By now, additional information about RAF and the corresponding T_g(RAF) must be known.

Figure 12 gives information about melting of crystals grown from the temperature region from T_g to T_m° . Crystals melting at low temperatures were earlier characterized as "annealing peaks".[5] The annealing peaks of PCL produced at a T_c in the marked glass transition range of Fig. 12 can be compared to the two-step nucleation data for iPS of Fig. 10 below approximately 400 K. The low-melting crystals of PCL were initiated by homogeneous nuclei produced below the temperature, where the originally present heterogeneous nuclei could initiate cold crystallization on analysis by heating, as shown in Fig. 11.

The lowest-melting, small PCL crystals seen in Fig. 12, grown in the glass transition range T_c = 185–225 K, give information about the structure and growth of the homogeneous nuclei out of which the small crystals must have grown. Once they melted, self-nuclei must have remained to move the cold crystallization on analysis to lower temperature than possible by the prior present heterogeneous nuclei. Three additional observations of importance were made in this low-temperature range of crystallization: (a) As the crystallization time, t_c, increases, T_p increases and ultimately reaches the line drawn in Fig. 12, indicating a continuous annealing after the path from nucleus to the initial crystal. (b) The heat of fusion of the crystals increased with time from zero (at t_c, <0.1 ms), but stops at less crystallinity than reached on subsequent cold crystallization. (c) Increasing t_c, leads to increasing RAF, so that by the time the straight-line in Fig. 12 has been reached, the ΔC_p at the glass transition indicates that *all* remaining amorphous phase is present as RAF and the sample has reached the *maximum semicrystallinity for the given* T_c. These observations of crystallization at the beginning of the glass transition seems to go parallel with homogeneous nucleation followed by crystallization modeled earlier parallel to the small molecule growth [8]: A critical nucleus of positive free enthalpy and nanophase dimension has to be overcome first by random fluctuation which then can lead to the increasingly larger crystals of microphase-dimension with a negative free enthalpy, governed in growth by its surface free energies. The rate of growth was assumed to slow down as the molecular motion slows, parallel with the increase of the viscosity when approaching the glass transition. The present, more detailed analysis, however, produces some discrepancies.

The two-step homogeneous nucleation in Fig. 10 delineate different temperature regions of homogeneous nucleation. The technique used to gain the data of Fig. 12 supplies the following details: Amorphous PCL crystallized at T_c below 240 K and analyzed by heating with 1,000 K s^{-1} displays the following two steps of transitions. First, there is the homogeneous nucleation followed by small crystal growth and annealing at T_c. On analysis, it shows a first, low-temperature melting peak T_p of 220–280 K. On continued heating during the analysis, self-nuclei are left behind after the melting and initiate cold crystallization between 230 and 275 K (which at the higher temperatures T_c overlap with the initial melting, T_p). The cold crystals melt subsequently with a second T_p of ≈310 K (corresponding to the new, higher T_c experienced during analysis, with a small high-temperature shoulder at 320–330 K do to annealing).

The next crystallization range of the amorphous PCL, between 260 and 330 K, shows for short times, t_c, only cold crystallization initiated during analysis by heterogeneous nucleation at 275–280 K, again melting ultimately at 310–330 K. At longer times, t_c, homogeneous nucleation is noted at T_c which leads to increasing amounts of larger crystals with a melting peak of 340–365 K (with lesser or no cold crystallization on heating, similarly as seen in Fig. 11 after slower prior cooling). For all three crystallization regions the ultimate T_p fits approximately the same straight line of $T_p = T_c + 40$ K in Fig. 12. Similarly, activation diagrams for nucleation and crystallization rates covering 20 orders of magnitude starting at the beginning of the glass transition show a single mechanism for crystallization, but a double mechanism for nucleation.

Returning to the classical nucleation and growth description developed for small molecules, one must, when based on these experiments, develop a new model for

[5] Wunderlich [8], vol III, p. 191: "Another general observation is the occurrence of a small melting peak several degrees above the crystallization temperature. This melting peak has also been called "annealing peak" and is often interpreted as resulting from much poorer crystals growing between the larger crystals (polypropylene, polystyrene, nylons, and polyurethanes)." For examples see graphs of Figs. IX.22, 23, 24, 27, 31 in this reference.

flexible macromolecules. In the discussion of the glass transition for PE with Fig. 3, it was suggested that the basic *cis–trans*, large-amplitude motion is connected with the glass transition as well as the motion of the basic motif involved in formation of the critical nucleus and the further crystal growth. The data for PE, however, showed that this motion begins as a "local motion" at low temperature and gets gradually excited further at higher temperature with the more abrupt change of ΔC_p to "cooperative motion." These two stages must have different mechanisms and are governed by different viscosities. For PE, the beginning of these two stages of the glass transition were separated by $\approx$150 K. For other polymers a guess can be made from the distance from the beginning to the end of ΔC_p in the glass transition range to be as little as $\approx$15 K.

While all initially growing species for PCL at low temperature are crystalline [47], similar experiments with iPP at sufficiently low temperature lead to a metastable mesophase [50]. The mesophase (condis phase) has the same helix as the crystal (2 * 3/1), but contains disorder (conformational defects, also called ambidextrons, causing helix segments of the wrong handedness) [49]. Again, small mesophase particles grow at a T_c below the temperature where the originally present heterogeneous nuclei could have initiated cold ordering. The small particles, grown by homogeneous nucleation and ordering disorder on heating at a low enough temperature that the newly produced melt could be self-nucleated, followed by cold-mesophase-ordering, and at a sufficiently higher temperature, melting again, as seen for PCL [47].

This *second part of the* "*Solutions*" leads to the conclusion that the ordering of semicrystalline polymers stops as soon as the amorphous RAF hinders the addition of motifs to the crystal or mesophases. The level the RAF reached varies with ordering temperature and the nature of the ordered as well as the amorphous phase. Without assessing the RAF, the crystallization and melting of a given semicrystalline polymer cannot be understood. The study of the homogeneous nucleation in the vicinity of the glass transition shows that the slow-down of the nucleation can be governed either by the local large-amplitude motion, which freezes only at the low-temperature region of the glass transition, or already by the cooperative large-amplitude motion which freezes already in the high-temperature region of the glass transition. The overall diffusion slowing nucleation, thus, has two potential energy barriers. The irreversible free energy landscape describing the path from the amorphous phase to the ordered phase, thus, must be studied separately for each macromolecule and incorporate the short and long-range diffusion effects. The evaluation of the changing endotherm with t_c by DFSC may even allow the quantitative determination of the irreversible free energy landscape as a function of temperature.

Segregation on ordering

Despite that in the summary of the first part of the "Solutions" it was concluded that the ordering of flexible polymers is irreversible, a distribution of molecules segregates on crystallization. This was illustrated for the orthorhombic phase of PE in Fig. 8. Curve "3" indicates that the supercooling calculated from the equilibrium melting does not go parallel with such segregation, so that the observed fractionation cannot be based on the thermodynamic functions of crystallization. Similarly, Fig. 7 and the curve "4" in Fig. 8 prove that chain folding is not connected with the observed segregation. Based on these experiments, the cause of the non-equilibrium segregation was called "molecular nucleation" [35]. Today, this process is still not fully understood. In this "Section," several earlier observations of molar mass effects on ordering are reviewed and then combined to a likely third part of the "Solutions."

The nucleation experiments illustrated with Figs. 10, 11 and 12 for iPS and PCL, more than one diffusion-controlled nucleation effect, particularly when close to the glass transition, which can affect molecules of varying lengths differently. Such processes with different rates of ordering for molecules of different length maybe at the root of segregation. To gain more information, experiments about the molar mass dependence need to be analyzed with DFSC that has recently become available [51].

No remaining measurable latent heats have been recorded for the *self-nuclei produced at high temperature*. The nuclei were limited in number and survived heating above T_m° for measurable limits in temperature and time, but their number did not change on cooling to T_c. These observations suggest a certain dependence on molar mass, but they contribute little to the understanding of overall segregation on crystallization. Although the self-nuclei from solutions of PE could be identified as a high-molar mass, nodular entity [42, 43], they must have been created by their original crystallization and may at best be sorted by the zero-entropy-production melting, but then could apply only to the small percentage of the sample contained in the nuclei. Molecular nucleation, as seen in Fig. 8, however, applies to the majority of the crystal growth.

The number, size, and rate of *self-nuclei produced at low temperature* are also temperature dependent, particularly when created in the low-temperature region of the glass transition. Owing to the changing cooperativeness of the large-amplitude motion, the size of these self-nuclei is molar-mass dependent [47, 50, and 51]. When studying the growth of the small, low-melting, ordered crystals, or mesophase particles, one finds that they are connected with the formation of a sizable amount of RAF, limiting the overall ordering to a small percentage of the sample

(<10%). The properties of these ordered particles also changed with T_c. At the lowest T_c, they leave no low-temperature self-nuclei for cold ordering on subsequent heating. At higher T_c, they do leave active self-nuclei, but produce less RAF. At intermediate T_c, properties of both types can interfere. When T_c exceeds T_g, the low-melting particles remain stable beyond the cold ordering temperature [50]. From these surprising observations, one might suggest that before and during ordering on a larger scale, molecules aggregate by large-distance diffusion. Separated, smaller molecules may be able to order faster at lower temperatures than larger ones. These suggestions point to the need to inspect the molecular structure and their large-amplitude motion in the melt and solution before and during ordering.

In analogy to an ideal gas, one can visualize an ideal, "gaseous," amorphous, flexible macromolecule by filling a vacuum with random coils of the molecules. To change to a real molecule, it would then have to be expanded by the hindering of the random rotation as a function of its rotation angle (hindered rotation) and by the volume excluded by the other parts of the same molecule and, if present, by solvent molecules.[6] In the melt, the various molecules would interpenetrate, and in solution, they could be increasingly separated by reducing the polymer concentration. *Single-molecule particles* of atactic PS, PE, and POE could be seen by electron microscopy or scanning force microscopy after growth from solutions of different concentrations by techniques ranging from precipitation at different rates, to freeze drying, and even electrospraying [52, 53].

The well-characterized PE molecules A–C shown in Fig. 5 were dissolved in *p*-xylene (polymer concentration of 1.0 wt%), and to produce poor crystals, they were quenched at $\approx$10 K s^{-1}. As parts of larger dendrites, approximately single-molecule crystal segments could be identified by their size. To judge molar mass segregation, the highest melting crystals of all samples were determined by DSC. For sample C, the end of melting agreed within −0.2 K with the computed zero-entropy-production melting temperature of the single-molecule single-crystal. For samples B and A, the deviations were +10 and +49 K, respectively, meaning that the lower molar mass molecules had (laterally) aggregated under the same crystallization conditions [53]. These data are the first indications that the shorter molecules could undergo longer distance diffusion to grow (laterally) into bigger crystals than the larger molecules.

When the polymer concentration was sufficiently small to avoid overlap of the molecules, the particle-size distribution of atactic PS could be matched with the molar mass distribution determined by size-exclusion chromatography. Single-molecule, folded-chain POE single crystals grown from a 2×10^{-4} wt% polymer solution could be identified by size and electron diffraction [53]. Finally, fractions of iPS single-molecule glassy particle were similarly produced and then crystallized from the melt at 448.2 K (see Fig. 10). Electron microscopy and diffraction revealed the formation of folded-chain, single-molecule, single-crystals [54]. The single-molecule particles did not grow to equilibrium either, i.e., their molecular separation hindered only the diffusion to create large crystals. The crystals were still chain folded, similar to the flexible macromolecules grown from bulk, i.e., they reached only a metastable state as summarized in parts 1 and 2 of the "Solutions."

The *third part of the* "*Solutions*" is presently not fully resolved. The study of the mechanism involving "self-nuclei produced at low temperature" did not identify a molecular nucleation process. It would be necessary to account for the fact that polymer molecules which only have a difference of thermodynamic driving force of a kelvin or less in equilibrium melting temperature are segregated at the crystal surface when growing as much as 5 K *below* T_m° (see Fig. 8). This observation seems to leave long-range diffusion of whole molecules to the crystal growth face as the only process to govern segregation.

Some more details can be extracted from the study of the "single-molecule particles." Indeed, shorter molecules can under similar crystallization condition grow into aggregates of thousands of molecules, while molecules of with $\approx$100 times higher mass average molar mass grow as single-molecule single-crystals (samples A and C of Fig. 8). To understand these enormous changes, one must remember the basic motif for ordering flexible macromolecules, the "bead" is less than 1 nm in length, while the overall molecule may be 25-μm long (PE of 300,000 Da molar mass) and the time scale for conformational motion is less the 10^{-12} s [24, see footnote 6]. One may speculate, thus, that diffusion on a motif-scale is involved in the basic ordering steps (giving a nodular morphology for the ordered macromolecules, of type D of Fig. 4) while to grow large crystals, many molecules must be assembled involving long-distance diffusion. The long-distance diffusion is also the process involved in the intrinsic viscosity of polymer melts and solutions and leads on ordering to spherulitic morphology which needs the development of a largely different model of crystal growth as was developed for small-molecule single-crystals.

Conclusions

Semicrystalline polymers have two major reasons for metastability. On irreversible crystallization or ordering,

[6] See: 1.3: chain statistics of macromolecules, and 1.4: size and shape measurement [9].

RAF is produced and prohibits the completion of crystallization. Depending on the nature of the polymer, different degrees of RAF are created. The nature and amount of the RAF are measurable by assessing the molecular motion, for example by evaluating ΔC_p throughout the glass transition region. The ordered phases, in contrast, can be assessed by measuring the latent heats throughout the ordering or disordering regions. The second reason for metastability is the chain folding, based on the chain-folding principle which prohibits direct chain extension for most crystals. For the mesophases, liquid crystals usually have are little hindered to extend the chains to equilibrium size. For condis crystals, chain extension of the more flexible molecules is observed as part during the common annealing process after initial ordering. Under proper condition, equilibrium crystals can be produced from the metastable crystals by removal of the partial crystallinity and chain folding. The melting of the metastable as well as equilibrium crystals can be described by zero-entropy production paths using irreversible and equilibrium thermodynamics, respectively.

The remaining problem is the understanding of the observed segregation of molar mass during the irreversible ordering path. Several processes may be linked to understand this problem. They involve long-range diffusion (which must be separated from the less molar-mass dependent short-range diffusion). The study of self-nucleation, molecular nucleation, and the growth of single-molecule, single-crystals have given some information about the steps involved in the segregation processes. The newly developed DFSC, capable of quenching metastable states for subsequent analysis, may be able to resolve these problems in the near future if applied to properly selected samples.

References

1. Wunderlich B. Thermal analysis of materials. A computer-assisted lecture course, published via the Internet (2005–2007). http://www.scite.eu and http://athas.prz.rzeszow.pl. Copyright: 16 Jan 2007.
2. Prime RB, Wunderlich B. Extended-chain crystals. III. Size distribution of polyethylene crystals grown under elevated pressure. J Polym Sci A-2. 1969;7:2061–72.
3. Prime RB, Wunderlich B. Extended-chain crystals. IV. Melting under equilibrium conditions. J Polym Sci A-2. 1969;7:2073–89. [Partially preprinted under the title: "The equilibrium melting of polymers," and presented at the Proc. IUPAC symp in Kyoto and Tokyo, Japan, 30 Sep 1966].
4. Prime RB, Wunderlich B, Melillo L. Extended-chain crystals. V. Thermal analysis and electron microscopy of the melting process in polyethylene. J Polym Sci A-2. 1969;7:2091–7.
5. Flory PJ. Thermodynamics of crystallization of high polymers. IV. A theory of crystalline states and fusion in polymers, copolymers, and their mixture with diluents. J Chem Phys. 1949;17:223–40.
6. Wunderlich B. The melting of defect polymer crystals. Polymer. 1964;5:611–24.
7. Wunderlich B. Crystallization during polymerization. Fortschr Hochpolymeren Forsch. Adv Polym Sci. 1968;5:568–619.
8. Wunderlich B. Macromolecular physics, vol I (crystal structure, morphology, defects, Chap 1–4), vol II (crystal nucleation, growth, annealing, Chap 5–7), vol III (crystal melting. Chap 8–10). New York: Academic Press; 1973, 1976, and 1980. http://www.scite.eu and http://athas.prz.rzeszow.pl.
9. Wunderlich B. Thermal analysis of polymeric materials. Berlin: Springer; 2005. ISBN 978-3-540-23629-0. www.springer.com/3-540-23629-5.
10. Dalton J. A new system of chemical philosophy. London; 1808.
11. The term 'macromolecule' was first used on p 788 of: Staudinger H, Fritschi J. Über die Hydrierung des Kautschuks und über seine Konstitution. Helv Chim Acta 1922;5:785–806.
12. Staudinger H. Arbeitserinnerungen. Heidelberg: Hüthig; 1961. In his Nobel Lecture of 1953 Staudinger sets the limit of small molecules at 1,000 atoms (p. 317).
13. Chen W, Wunderlich B. Nanophase separation of small and large molecules. Macromol Chem Phys. 1999;200:283–311.
14. Wunderlich B. Thermodynamic description of condensed phases. J Therm Anal Calorim. 2010;102:413–24.
15. Wunderlich B. Study of the change in specific heat of monomeric and polymeric glasses during the glass transition. J Phys Chem. 1960;64:1052–6.
16. Hildebrand JH. The entropy of vaporization as a means of distinguishing normal liquids. J Am Chem Soc. 1915;37:970–8.
17. See, for example: Herzberg G. Infrared and Raman spectra of polyatomic molecules. Princeton: van Nostrand; 1945.
18. Wunderlich B. The glass transition as key to identify solid phases. J Appl Polym Sci. 2007;105:49–59.
19. Einstein A. Die Plancksche Theorie der Strahlung und die Theorie der spezifischen Wärme. Ann Phys. 1907;22:180–190 (corrections p. 800).
20. Debye P. Zur Theorie der spezifischen Wärme. Ann Phys. 1912;39:789–839.
21. Wunderlich B, Baur H. Heat capacities of linear high polymers. Fortschr Hochpolymeren Forsch. Adv Polym Sci. 1970;7:151–368.
22. Gaur U, Wunderlich B. The glass transition temperature of polyethylene. Macromolecules. 1980;13:445–6.
23. Wunderlich B. The Athas Data Base on heat capacities of polymers. Pure Appl Chem 1995;67:1019–1026. For data tables see Pyda M http://athas.prz.rzeszow.pl.
24. Sumpter BG, Noid DW, Liang GL, Wunderlich B. Atomistic dynamics of macromolecular crystals. Adv Polym Sci. 1994;116:27–72.
25. Wunderlich B, Poland D. Thermodynamics of crystalline linear high polymers. II. The influence of copolymer units on the thermodynamic properties of polyethylene. J Polym Sci A. 1963;1:357–72.
26. Suzuki H, Grebowicz J, Wunderlich B. The glass transition of polyoxymethylene. Br Polym J. 1985;17:1–3.
27. Sullivan P, Wunderlich B. The interference microscopy of crystalline linear high polymers. SPE Trans. 1964;1964(4):113–9.
28. Pak J, Wunderlich B. Reversible melting of polyethylene extended-chain crystals detected by temperature-modulated calorimetry. J Polym Sci B Polym Phys. 2002;40:2219–27.
29. Hellmuth E, Wunderlich B. Superheating of linear high-polymer polyethylene crystals. J Appl Phys. 1965;36:3039–44.
30. Pak J, Boller A, Moon I, Pyda M, Wunderlich B. Thermal analysis of paraffins by calorimetry. Thermochim Acta. 2000;357/358:259–66.
31. Pak J, Wunderlich B. Melting and crystallization of polyethylene of different molar mass by calorimetry. Macromolecules. 2001;34:4492–503.

32. Wunderlich B. Reversible crystallization and the rigid-amorphous phase in semicrystalline macromolecules. Prog Polym Sci. 2003;28(3):383–450.
33. Mehta A, Wunderlich B. A study of molecular fractionation during the crystallization of polymers. Colloid Polym Sci. 1975;253:193–205.
34. Wunderlich B, Mehta A. Macromolecular nucleation. J Polym Sci Polym Phys Ed. 1974;12:255–63.
35. Wunderlich B. Molecular nucleation and segregation. Faraday Discuss R Soc Chem. 1979;68:239–43.
36. Mehta A, Wunderlich B. Detection of tie-molecules by thermal analysis. Makromol Chem. 1974;175:977–82.
37. Wunderlich B. Calorimetry of nanophases of macromolecules. Int J Thermophys. 2007;28:958–67.
38. Pak J, Pyda M, Wunderlich B. Rigid amorphous fractions and glass transitions in poly(oxy-2,6-dimethyl-1,4-phenylene). Macromolecules. 2003;36:495–9.
39. Cheng SZD, Wunderlich B. Glass transition and melting behavior of poly(oxy-2,6-dimethyl-1,4-phenylene). Macromolecules. 1987;20:1630–7.
40. Kunz M, Möller M, Heinrich U-R, Cantow H-J. Electron spectroscopic imaging studies on polyethylene, chain-folded and extended-chain crystals. Makromol Chem Makromol Symp. 1988;20(21):147–58.
41. Wunderlich B. The influence of liquid to solid transitions on the changes of macromolecular phases from disorder to order. Thermochim Acta. 2011;522:2–13.
42. Blundell DJ, Keller A, Kovacs AJ. A new self-nucleation phenomenon and its application to the growing of polymer crystals from solution. J Polym Sci B. 1966;4:481–6.
43. Blundell DJ, Keller A. Nature of self-seeding polyethylene crystal nuclei. J Macromol Sci. 1968;b2:301–36.
44. Boon J, Challa G, Van Krevelen DW. Crystallization kinetics of isotactic polystyrene II Influence of thermal history on number of nuclei. J Polym Sci A-2 Polym Phys Ed. 1968;6:1835–51.
45. Koutsky JA, Walton AG, Baer E. Nucleation of polymer droplets. J Appl Phys. 1967;38:1832–9.
46. Zhuravlev E, Schick C. Fast scanning power compensated differential scanning nano-calorimeter: 1. The device. Thermochim Acta. 2010;50:1–13.
47. Zhuravlev E, Schmelzer JWP, Wunderlich B, Schick C. Kinetics of nucleation and overall crystallization in poly(ε-caprolactone) (PCL). Polymer. 2011;52:1863–997.
48. Pyda M, Nowak-Pyda E, Heeg J, Huth H, Minakov AA, Di Lorenzo ML, Schick C, Wunderlich B. Melting and crystallization of poly(butylene terephthalate) by temperature-modulated and superfast calorimetry. J Polym Sci B Polym Phys. 2006;44:1364–77.
49. Androsch R, Di Lorenzo ML, Schick C, Wunderlich B. Mesophases in polyethylene, polypropylene and poly(1-butene). Polymer. 2010;51:4639–62.
50. Mileva D, Androsch R, Zhuravlev E, Schick C, Wunderlich B. Homogeneous nucleation and mesophase formation in glassy isotactic polypropylene. Polymer. 2012;53:277–82.
51. Wurm A, Zhuravlev E, Eckstein K, Jehnichen D, Pospiech D, Androsch R, Wunderlich B, Schick C. Crystallization and homogeneous nucleation kinetics of poly(ε-caprolactone) (PCL) with different molar masses. Macromolecules (submitted).
52. Festag R, Alexandratos SD, Cook KD, Joy DC, Annis B, Wunderlich B. Single- and few-chain polystyrene particles by electrospray. Macromolecules. 1997;30:6238–42.
53. Bu H, Pang Y, Song D, Yu T, Voll TM, Czornyj G, Wunderlich B. Single molecule single crystals. J Polym Sci B Polym Phys. 1991;29:139–52.
54. Bu H, Chen E, Xu S, Guo K, Wunderlich B. Single-molecule single crystals of isotactic polystyrene. J Polym Sci B Polym Phys. 1994;32:1351–7.